



An HER3-targeting antibody–drug conjugate incorporating a DNA topoisomerase I inhibitor U3-1402 conquers EGFR tyrosine kinase inhibitor-resistant NSCLC

Kimio Yonesaka¹ · Naoki Takegawa¹ · Satomi Watanabe¹ · Koji Haratani¹ · Hisato Kawakami¹ · Kazuko Sakai² · Yasutaka Chiba³ · Naoyuki Maeda⁴ · Takashi Kagari⁵ · Kenji Hirotsu⁶ · Kazuto Nishio² · Kazuhiko Nakagawa¹

Received: 24 August 2017 / Revised: 26 August 2018 / Accepted: 4 September 2018
© Springer Nature Limited 2018

Abstract

EGFR tyrosine kinase inhibitors (TKIs) are standard therapy for EGFR-mutant non-small cell lung cancer (NSCLC); however, these tumours eventually acquire chemoresistance. U3-1402 is an anti-HER3 antibody–drug conjugate with a novel topoisomerase I inhibitor, DXd. In the current study, we evaluated the anticancer efficacy of U3-1402 in EGFR-mutant NSCLC cells with acquired resistance to EGFR-TKIs. HCC827GR5 and PC9AZDR7 are EGFR-TKI-resistant clones for gefitinib and osimertinib, respectively. U3-1402 alone or in combination with the EGFR-TKI erlotinib demonstrated potent anticancer efficacy in HCC827GR5 cells using an *in vitro* growth inhibition assay and *in vivo* xenograft mouse model. U3-1402 induced apoptosis in HCC827GR5 cells accompanying phosphorylation of histone H2A.X, a marker of DNA damage, but did not block HER3/PI3K/AKT signalling. Further, we found using flow cytometry that the cell surface HER3 expression level in HCC827GR5 cells was twice that found in HCC827 cells, indicating internalization of U3-1402 was increased in resistant cells. In addition, administration of U3-1402 notably repressed growth of EGFR-TKI osimertinib-resistant PC9AZDR7 xenograft tumours, and that PC9AZDR7 cells expressed five times greater cell surface HER3 than PC9 cells. Furthermore, using immunofluorescent microscopy, HER3 was observed predominantly in the nucleus of PC9 cells, but was localized in the cytoplasm of PC9AZDR7 cells. This finding indicates that altered trafficking of the HER3-U3-1402 complex may accelerate linker payload cleavage by cytoplasmic lysosomal enzymes, resulting in DNA damage. Our results indicate that administration of U3-1402 alone or in combination with an EGFR-TKI may have potential as a novel therapy for EGFR-TKI-resistant EGFR-mutant NSCLC.

Electronic supplementary material The online version of this article (<https://doi.org/10.1038/s41388-018-0517-4>) contains supplementary material, which is available to authorized users.

✉ Kimio Yonesaka
yonesaka@med.kindai.ac.jp

- ¹ Department of Medical Oncology, Kindai University Faculty of Medicine, Osaka-Sayamashi, Osaka, Japan
- ² Department of Genome Biology, Kindai University Faculty of Medicine, Osaka-Sayamashi, Osaka, Japan
- ³ Clinical Research Center, Kindai University Hospital, Osaka-Sayamashi, Osaka, Japan
- ⁴ Biomarker Department, Daiichi Sankyo Co., Ltd., Shinagawa-ku, Tokyo, Japan
- ⁵ Biologics & Immuno-Oncology Laboratories, Daiichi Sankyo Co., Ltd., Shinagawa-ku, Tokyo, Japan
- ⁶ Oncology Clinical Development Department, Daiichi Sankyo Co., Ltd., Shinagawa-ku, Tokyo, Japan

Introduction

HER3 (also known as ERBB3) is a member of the human epidermal growth factor receptor (HER) family of receptor tyrosine kinases [1]. HER3 is aberrantly upregulated in some cancers such as non-small cell lung cancer (NSCLC) [2, 3]. Owing to structural features that limit its intrinsic kinase activity, HER3 cannot be auto-phosphorylated but can be trans-phosphorylated through coupling with other family members. Highly activated HER3 is observed in NSCLC with somatic mutations in the tyrosine kinase domain of epidermal growth factor receptor (EGFR) [4]. Mutated EGFR potently trans-phosphorylates HER3 upon binding and activated HER3 mediates the phosphatidylinositol-3 kinase (PI3K)/protein kinase B (AKT) cell survival signalling pathway. Thus, EGFR tyrosine kinase inhibitors (TKIs) can prevent HER3/PI3K/AKT signalling activation and achieve potent antitumour

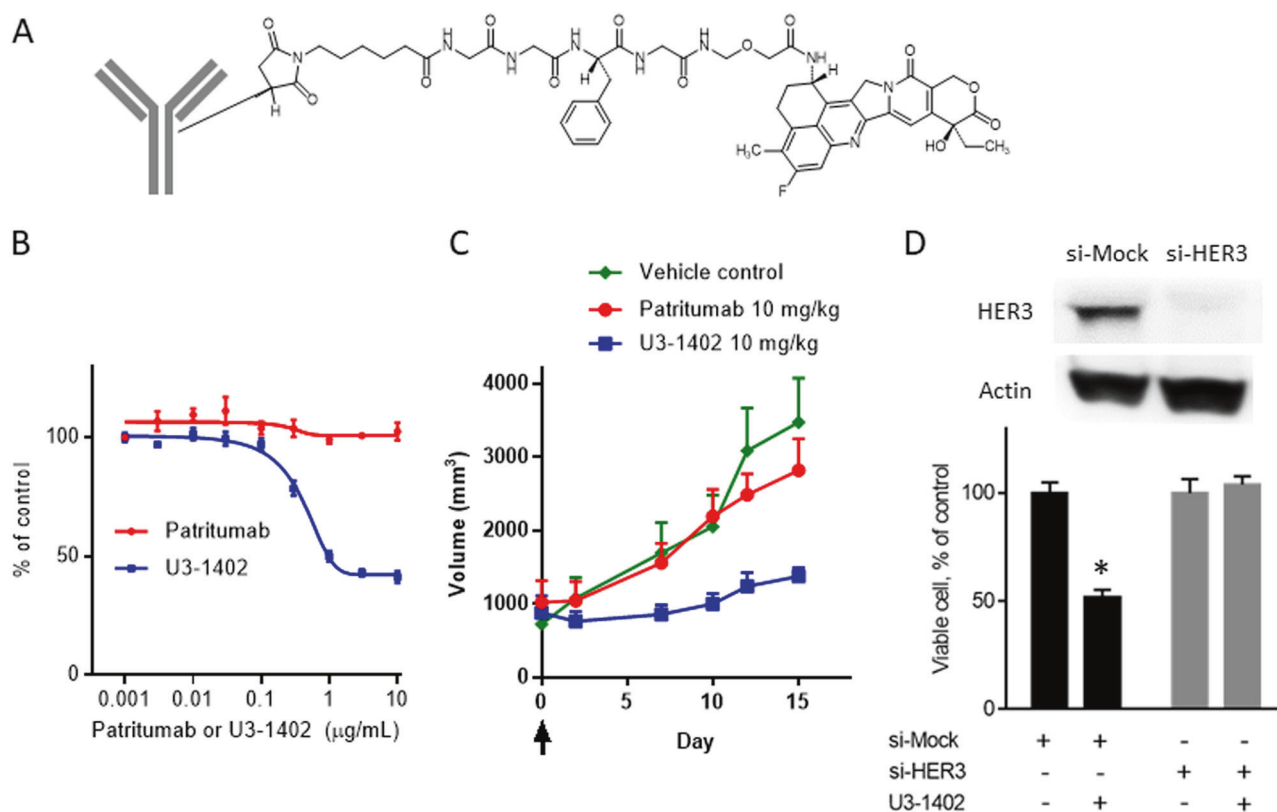


Fig. 1 **a** The structure of U3-1402. U3-1402 is composed of an anti-HER3 antibody and a derivative of DX-8951 (DXd), a topoisomerase I inhibitor, which are bound together by a GGFG peptide linker. The linker payload is conjugated with the antibody via the cysteine residues after the interchain disulphide bonds are reduced with a reducing agent. **b** In vitro growth inhibition assay for patritumab or U3-1402. HCC827GR5 cells were treated with the indicated concentrations of patritumab or U3-1402 for 7 days; cell viability was evaluated using the CellTiter-Glo viability assay and is shown relative to

untreated control cells (mean \pm SD of six independent experiments). **c** In a xenograft HCC827GR5 mouse model, tumours were treated with patritumab, U3-1402, or vehicle. Each treatment group consisted of six mice. Data represent mean \pm SEM. The vertical arrow indicates drug administration. **d** HCC827GR5 cells were transfected with si-HER3 or si-Mock. Immunoblotting was performed for detecting indicated proteins. Cells were treated with 1 μ g/mL U3-1402 for 3 days, and then cell viability was evaluated

activity in EGFR-mutant NSCLC [4]. Furthermore, HER3 plays a key role in EGFR-TKI resistance [5–7]. Amplification of the *MET* oncogene induces HER3 activation via coupling, thereby maintaining activation of the PI3K/AKT cell survival signalling pathway despite ongoing EGFR-TKI treatment [5]. These characteristics of HER3 and its role in cell survival suggest that HER3 is a promising therapeutic target for EGFR-mutant NSCLC.

Prior clinical trials have developed a number of anti-HER3 monoclonal antibodies [8–10]. U3-1287 (patritumab) is a fully human monoclonal antibody directed against the extracellular domain of human HER3 [6]. We previously demonstrated that the antitumour activity of patritumab in NSCLC correlated with the expression level of the HER3 ligand, heregulin, but not with HER3 expression [6]. Moreover, aberrant heregulin-expressing NSCLC exhibited highly activated HER3, which was severely reduced by patritumab treatment [6]. In contrast, patritumab could not inhibit the proliferation of EGFR-mutant NSCLC [6].

Indeed, cotreatment of patritumab with erlotinib had limited antitumour activity in patients with EGFR-mutant NSCLC with post-acquired EGFR-TKI resistance [11]. Therefore, an alternative HER3-targeting strategy is required for EGFR-mutant NSCLC treatment.

U3-1402 is a novel HER3-targeting antibody–drug conjugate (ADC) currently under clinical development [12]. U3-1402 is composed of an anti-HER3 antibody (patritumab) and a derivative of DX-8951 (DXd), which is a topoisomerase I inhibitor, bound together by a maleimide-GGFG peptide linker (Fig. 1a). U3-1402 is cleaved by lysosomal enzymes such as cathepsins B and L, releasing DXd, which inhibits topoisomerase I specifically in cancer cells, as U3-1402 binds to aberrantly expressed HER3 in cancer cells [12]. Furthermore, the unique linker-payload system reduces the ADC hydrophobicity, achieving a drug-to-antibody ratio (DAR) of eight for DXd, compared with DARs of 2–4 in other ADCs [12–14].

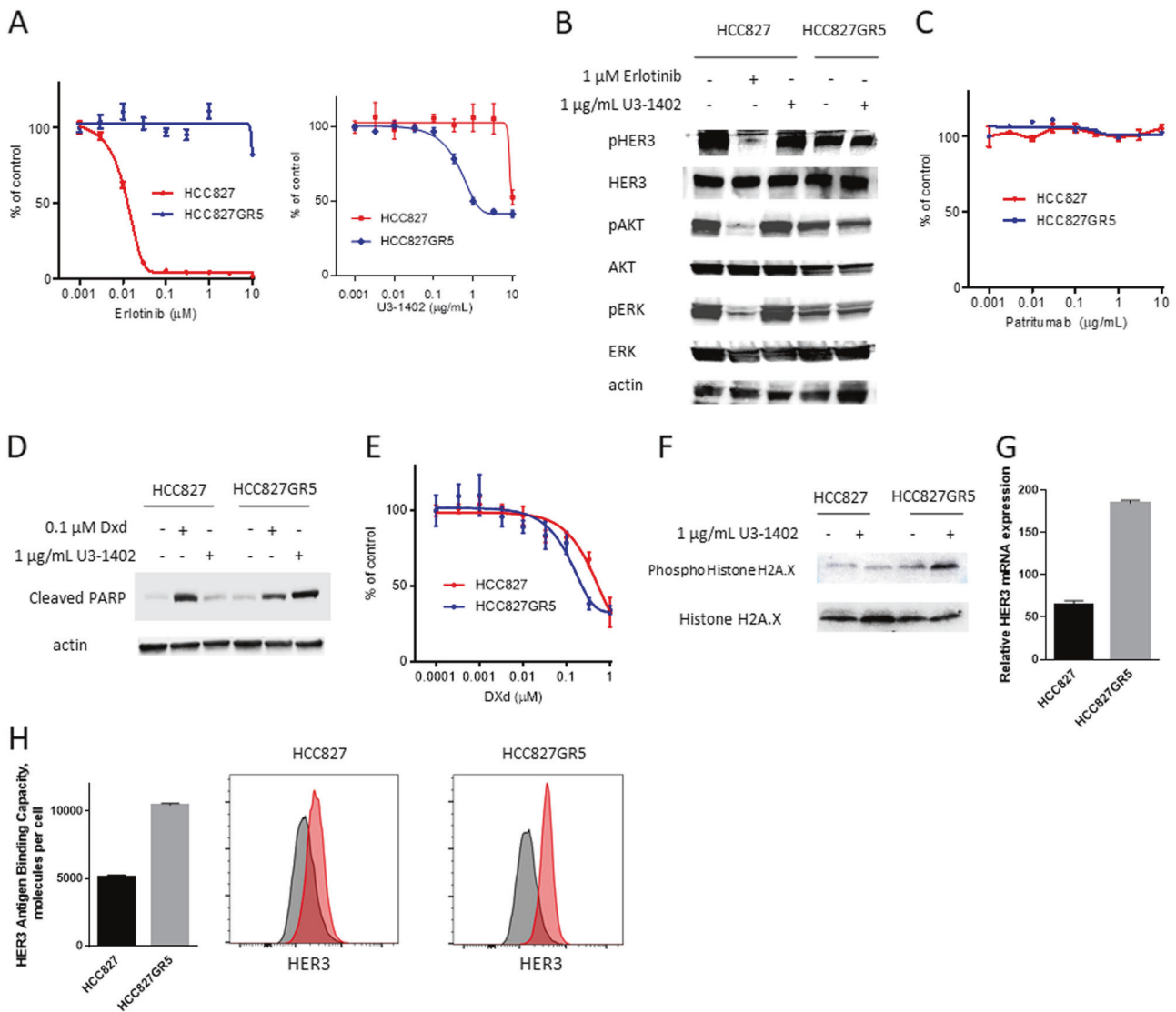


Fig. 2 **a** In vitro growth inhibition assay for Erlotinib or U3-1402. HCC827 or HCC827GR5 cells were treated with the indicated concentrations of Erlotinib or U3-1402 for 7 days; cell viability was evaluated using the CellTiter-Glo viability assay and is shown relative to untreated control cells (mean ± SD of six independent experiments). **b** HCC827 or HCC827GR5 cells were treated with 1 μM Erlotinib or 1 μg/mL U3-1402 for 6 h and then probed for the indicated proteins. **c** HCC827 or HCC827GR5 cells were treated with the indicated concentrations of Patritumab for 7 days; cell viability was evaluated using the CellTiter-Glo viability assay and is shown relative to untreated control cells (mean ± SD of six independent experiments). **d** HCC827 or HCC827GR5 cells were treated with 0.1 μM DXd or 1 μg/mL U3-

1402 for 3 days and then probed for the indicated proteins. **e** HCC827 or HCC827GR5 cells were treated with the indicated concentrations of DXd for 3 days; cell viability was evaluated using the CellTiter-Glo viability assay and is shown relative to untreated control cells (mean ± SD of six independent experiments). **f** HCC827 or HCC827GR5 cells were treated with 1 μg/mL U3-1402 for 6 days and then probed for the indicated proteins. **g** mRNA was obtained from HCC827 and HCC827GR5 cells, and *HER3* mRNA expression was analysed (mean ± SD of three independent experiments). **h** Cell surface HER3 expression in HCC827 and HCC827GR5 cells was measured by flow cytometry (mean ± SD of three independent experiments)

First- or second-generation EGFR-TKIs are standard first-line therapy for advanced EGFR-mutant NSCLC [15]. Furthermore, the third-generation EGFR-TKI osimertinib is an optimal treatment for NSCLC with a secondary Thr790Met point mutation (T790M) in EGFR, which is a gatekeeper mutation for first- and second-generation EGFR-TKIs [16, 17]. Despite the high efficacies of EGFR-TKIs,

all tumours eventually acquire chemoresistance, and therefore, novel treatment strategies are necessary for treatment after acquired resistance to EGFR-TKIs. In the current study, we evaluated the anticancer efficacy of U3-1402 in EGFR-mutant NSCLC with acquired resistance to EGFR-TKIs and explored its underlying molecular mechanisms.

Results

Gefitinib-resistant HCC827GR5 cells resistant to patritumab but sensitive to U3-1402

We evaluated the anticancer efficacy of U3-1402 compared with that of patritumab in EGFR-TKI-resistant HCC827GR5 cells. HCC827GR5 is an isolated clone of gefitinib-resistant cells generated by continuous gefitinib exposure, and its resistance is due to *MET* genomic amplification [5]. Using an in vitro growth inhibition assay, HCC827GR5 cells were treated with patritumab or U3-1402 at doses of 0.0033–10 µg/mL for 7 days. As expected, cells viability was maintained in the presence of increasing concentrations of patritumab (Fig. 1b). In contrast, U3-1402 reduced cell viability in a dose-dependent manner (Fig. 1b).

To verify whether this could be observed in vivo, HCC827GR5 cells were implanted subcutaneously in mice, which were then treated with a single dose of patritumab (10 mg/kg), U3-1402 (10 mg/kg), or vehicle for 15 days. Growth of xenograft tumours was partially inhibited by patritumab with a treatment-to-control (T/C) ratio of 81% (Fig. 1c), while growth was significantly prevented by U3-1402 with a T/C ratio of 40%.

To confirm that the efficacy of U3-1402 depends on HER3 expression, we specifically inhibited HER3 in HCC827GR5 cells using HER3-targeted small interfering RNA (siRNA; si-HER3; Fig. 1d). In vitro growth inhibition assay showed that cells treated with mock siRNA were sensitive to U3-1402, whereas those treated with si-HER3 were resistant to U3-1402 (Fig. 1d). These results show that the HER3-targeted ADC U3-1402 exhibits enhanced anti-tumour efficacy compared with patritumab in vitro and in vivo, and this effect is HER3 dependent.

EGFR-TKI-resistant HCC827GR5 cells have increased susceptibility to U3-1402 compared with parent HCC827 cells

Considering that resistance to EGFR-TKI may influence the anticancer activity of U3-1402, we next compared the susceptibility of HCC827GR5 cells and their parent HCC827 cells with U3-1402 using an in vitro growth inhibition assay. Both cell lines were treated with the EGFR-TKI erlotinib at doses of 0.0033–10 µM or U3-1402 at doses of 0.0033–10 µg/mL for 7 days. Although HCC827GR5 cells markedly lost susceptibility to erlotinib compared with HCC827 parent cells, HCC827GR5 cells unexpectedly exhibited greater susceptibility to U3-1402 than their parent cells (Fig. 2a). Specifically, 1 µg/mL U3-1402 had no inhibitory effect on HCC827 cells but did inhibit proliferation in 50% of untreated HCC827GR5 cells. We hypothesized that this differing susceptibility was caused by stronger U3-1402-

induced inhibition of HER3-mediated PI3K/AKT cell signalling in HCC827GR5 cells compared with that in HCC827 cells, and we tested this hypothesis by immunoblot assay. The expression levels of total and phosphorylated HER3, its downstream effector AKT, and extracellular signal-regulated kinase (ERK) in both HCC827 cells and HCC827GR5 cells were determined following 3 h of treatment with either 1 µM erlotinib or 1 µg/mL U3-1402. In HCC827 but not HCC827GR5 cells, erlotinib treatment resulted in decreased phosphorylation of HER3, AKT, and ERK (Fig. 2b, Supplementary Figure S1). In contrast, no decreased phosphorylation of HER3, AKT, or ERK was detected in either HCC827 or HCC827GR5 cells following U3-1402 administration. Additionally, a similar growth inhibition assay was performed in HCC827 and HCC827GR5 cells with patritumab instead of U3-1402, but we did not observe any particular susceptibility to patritumab in these cell lines (Fig. 2c). These results suggest that the anticancer efficacy of U3-1402 in HCC827GR5 cells was not caused by HER3/PI3K/AKT signalling blockade.

HCC827GR5 cells exhibit greater surface expression of HER3 than HCC827 parent cells

Next, we evaluated apoptosis and DNA damage induced by topoisomerase I inhibition by detecting cleaved poly adenosine diphosphate-ribose polymerase (PARP) and phosphorylation of histone H2A.X as markers of apoptosis and DNA damage, respectively, in HCC827 and HCC827GR5 cells using an immunoblot assay. DXd at 0.1 µM comparably induced PARP cleavage in both HCC827 and HCC827GR5 cells (Fig. 2d). Additionally, using an in vitro growth inhibition assay, we evaluated the anti-proliferative activity of DXd in these cells at doses of 0.00033–1 µM for 3 days. We observed equivalent susceptibility to DXd in these cell lines, with IC₅₀ values of 0.74 µM and 0.6 µM for HCC827 and HCC827GR5, respectively (Fig. 2e). In contrast, 1 µg/mL U3-1402 induced PARP cleavage in only HCC827GR5 cells but not in HCC827 cells (Fig. 2d). Exposure to 1 µg/mL U3-1402 for 6 days increased the phosphorylation of histone H2A.X in HCC827GR5 cells but minimally changed the phosphorylation in HCC827 cells (Fig. 2f). In contrast, 0.1 µM DXd phosphorylated histone H2A.X to a similar extent in HCC827 and HCC827GR5 cells (Supplementary Figure S2). These results indicate that U3-1402 induces apoptosis to a greater extent in HCC827GR5 cells than in HCC827 cells depending on the extent of DNA damage, although both cell lines exhibited similar susceptibility to DXd.

We proposed that a cause for the differing susceptibilities to U3-1402 may be differences in the internalization ratios of the HER3-U3-1402 complex between these cell lines, and we hypothesized that a high ratio of HER3-U3-1402 complex

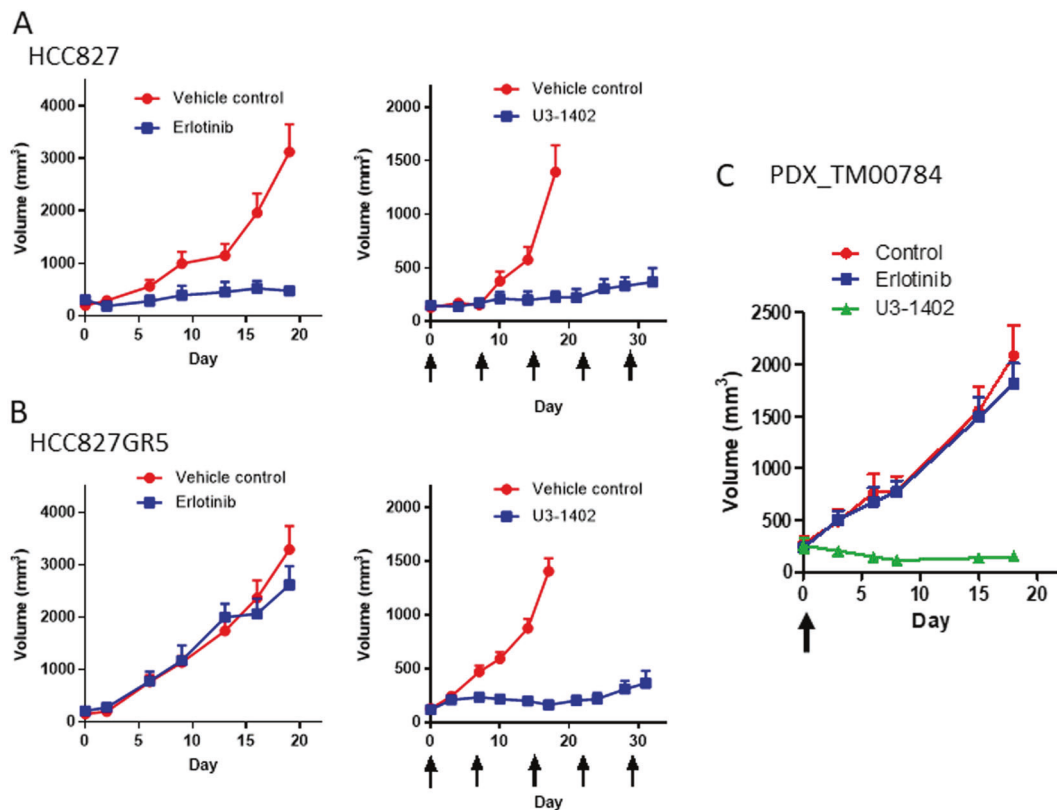


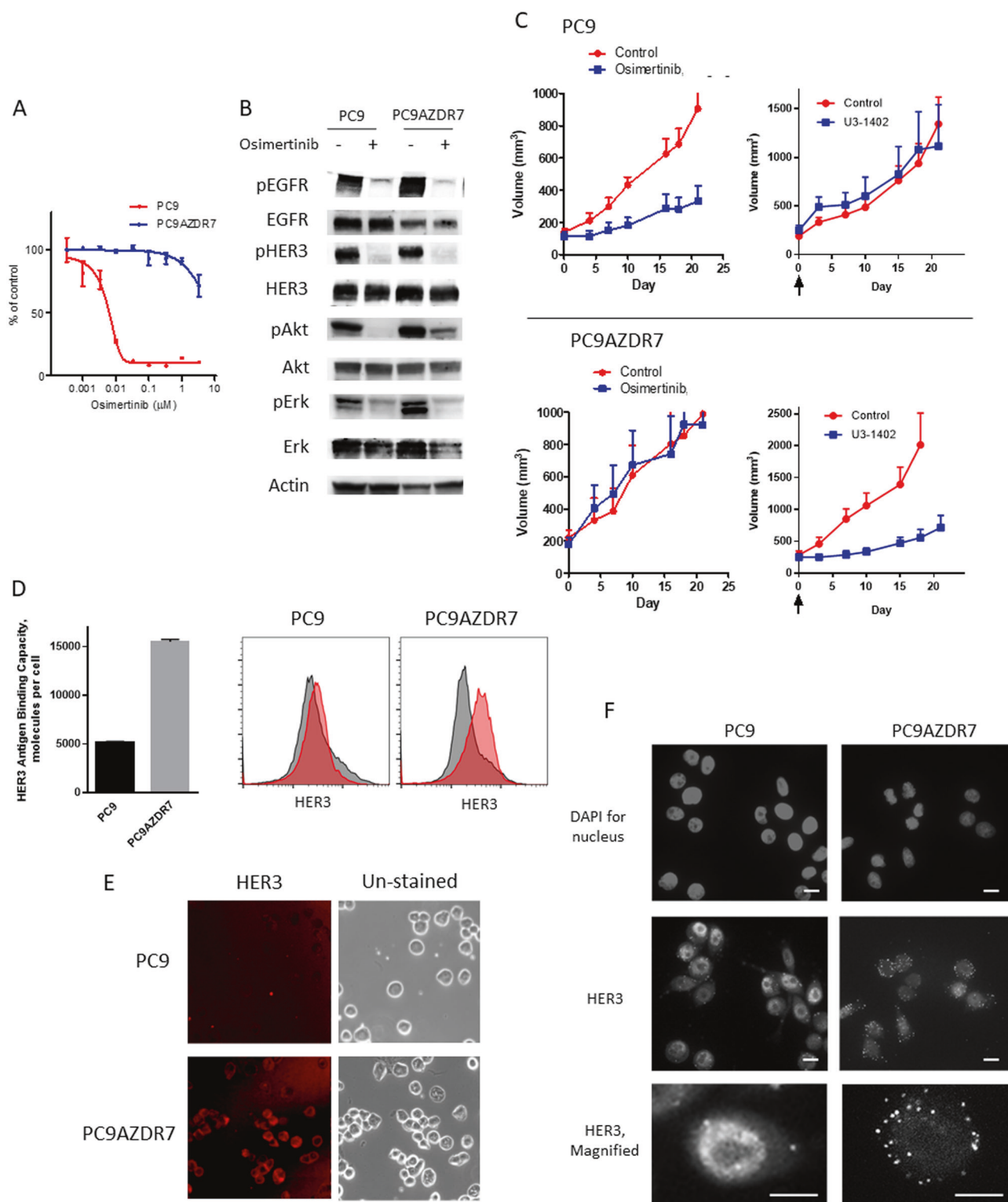
Fig. 3 In a xenograft **a** HCC827, **b** HCC827GR5, or **c** PDX mouse model, tumours were treated with erlotinib, U3-1402, or vehicle. Each treatment group consisted of eight mice. Data represent mean \pm SEM. The vertical arrow indicates drug administration

internalization would increase the intracellular concentration of DXd. Therefore, we measured *HER3* mRNA levels by quantitative real-time PCR (RT-PCR) and found that *HER3* levels were approximately three times higher in HCC827GR5 cells than in HCC827 cells (184.5 vs. 64.9, respectively, $p < 0.0001$; Fig. 2g). However, because mRNA levels do not always reflect the amount of protein, we used flow cytometry to measure levels of cell surface HER3, which may better correlate with the observed susceptibility to ADCs. HCC827GR5 cells had approximately twice as many HER3 molecules per cell than HCC827 cells (10,452 vs. 5144, respectively, $p < 0.0001$; Fig. 2h). Immunofluorescence staining also demonstrated greater cell surface HER3 expression in HCC827GR5 cells than in HCC827 cells (Supplementary Figure S3). These results indicate that greater HER3 cell surface expression may accelerate internalization of the HER3-U3-1402 complex, resulting in an increased concentration of DXd, which induces more apoptosis in HCC827GR5 cells than in HCC827 cells.

In vivo antitumour activity of U3-1402 in EGFR-TKI-resistant HCC827GR5 cells

To determine whether the anticancer efficacy of U3-1402 in HCC827GR5 cells applied in vivo, we compared the

anticancer efficacy of U3-1402 on HCC827GR5- and HCC827-derived xenograft tumours in mice. These cell lines were implanted subcutaneously in mice, which were then treated with daily oral (p.o.) administration of erlotinib (25 mg/kg), weekly intraperitoneal (i.p.) administration of U3-1402 (10 mg/kg), or vehicle for 19 or 31 days. On day 19, growth of the xenograft tumours from HCC827 parent cells was effectively prevented by administration of either erlotinib or U3-1402, with T/C ratios of 15 and 16%, respectively (Fig. 3a). In contrast, tumours originating from HCC827GR5 cells continued to grow despite erlotinib treatment with a T/C ratio of 79% on day 19 (Fig. 3b). However, growth of HCC827GR5-derived tumours was significantly impaired by treatment with U3-1402 on day 17 (T/C ratio of 12%; Fig. 3b). Additionally, we examined the efficacy of U3-1402 in a patient-derived xenograft (PDX) mouse model. A patient with NSCLC harbouring the EGFR L858R mutation was treated with erlotinib. A tissue sample was collected after disease progression on erlotinib treatment and was implanted in mice, which were then treated with daily oral (p.o.) administration of erlotinib (25 mg/kg), i.p. administration of a single dose of U3-1402 (5 mg/kg), or vehicle for 18 days. The PDX, TM00784, exhibited *MET* genomic amplification. TM00784 continued to grow despite erlotinib treatment with a T/C ratio of 87% on day



18 (Fig. 3c). However, growth of TM00784 was significantly impaired by treatment with U3-1402 on day 18 (T/C ratio of 7%; Fig. 3c). These results suggest that U3-

1402 exerts potent anticancer activity against EGFR-mutant tumours despite acquired resistance to first-generation EGFR-TKIs.

◀ **Fig. 4 a** In vitro growth inhibition assay for osimertinib. PC9 or PC9AZDR7 cells were treated with the indicated concentrations of osimertinib for 3 days; cell viability was evaluated using the CellTiter-Glo viability assay and is shown relative to untreated control cells (mean \pm SD of six independent experiments). **b** PC9 or PC9AZDR7 cells were treated with 100 nM osimertinib for 6 h and then probed for the indicated proteins. **c** In a xenograft PC9 or PC9AZDR7 mouse model, tumours were treated with erlotinib, U3-1402, or vehicle. Each treatment group consisted of eight mice. Data represent mean \pm SEM. The vertical arrow indicates drug administration. **d** Cell surface HER3 expression in PC9 and PC9AZDR7 cells was measured by flow cytometry (mean \pm SD of three independent experiments). **e** Cell surface HER3 expression in PC9 and PC9AZDR7 cells was analysed by immunofluorescent staining. **f** Immunofluorescent microscopy showing the intracellular localization of HER3 (anti-HER3) and the nucleus (DAPI) in PC9 and PC9AZDR7 cells. Scale bars indicate 10 μ m

Osimertinib-resistant PC9AZDR7 cells have greater sensitivity to U3-1402 than parent PC9 cells

To examine whether these findings from HCC827GR5 cells were relevant to other EGFR-TKI-resistant cancer cells, we evaluated U3-1402 anticancer efficacy using a cell line resistant to a third-generation EGFR-TKI, osimertinib. An osimertinib-resistant cell line was established by chronic exposure of PC9 cells to increased doses of osimertinib up to 100 nM (Supplementary materials and methods) [18]. We performed an in vitro growth inhibition assay using cells from PC9 or PC9AZDR7, a clone of these osimertinib-resistant cells, treated with osimertinib at doses of 0.001–3.3 μ M for 3 days. The results showed decreased viability of PC9 cells dependent on the osimertinib concentration, with an IC₅₀ value of 0.007 μ M (Fig. 4a). In contrast, PC9AZDR7 cells were resistant to osimertinib with an IC₅₀ value over 10 μ M (Fig. 4a). Similarly, other resistant clones exhibited resistance to 1 μ M osimertinib (Supplementary Figure S4). The observed resistance to osimertinib in the PC9AZDR7 clone line was maintained over time, even after 30 passages in osimertinib-free medium (Supplementary Figure S5). Furthermore, xenograft tumours arising from PC9 parent cells were sensitive to osimertinib (1 mg/kg), whereas those from PC9AZDR7 cells were resistant to 1 mg/kg (Fig. 4c) or 5 mg/kg osimertinib (Supplementary Figure S6) daily administration.

Next, we evaluated the effects of osimertinib on the phosphorylation of EGFR, AKT, and ERK1/2 in parental PC9 and PC9AZDR7 cells and observed that osimertinib effectively inhibited EGFR phosphorylation in both parental and drug-resistant cells (Fig. 4b). Consistent with these observations, no secondary mutations in EGFR were detected in PC9AZDR7 cells, and HER3 and downstream AKT phosphorylation were completely inhibited in PC9 cells (Fig. 4b). However, in contrast to the observations in parental PC9 cells, AKT phosphorylation in PC9AZDR7 cells was partially maintained following osimertinib

treatment, although HER3 phosphorylation was completely inhibited (Fig. 4b). Because osimertinib inhibited EGFR phosphorylation, EGFR is unlikely to be responsible for activation of the AKT signalling observed in PC9AZDR7 cells (Fig. 4b). In contrast to AKT, we found that ERK1/2 phosphorylation was inhibited in PC9AZDR7 cells (Fig. 4b), suggesting that EGFR still controls ERK1/2 signalling in PC9AZDR7 cells. We additionally examined the sensitivity of PC9AZDR7 cells to the AKT-specific inhibitor ipatasertib. PC9AZDR7 cells were completely resistant to 100 nM osimertinib, as shown in Supplementary Fig. S7. However, these cells partially recovered their sensitivity to osimertinib when combined with ipatasertib (Supplementary Fig. S7). These findings indicate that remnant AKT activation partially leads to cell survival under osimertinib treatment; thus, the resistance mechanism could not be fully elucidated in PC9AZDR7 cells.

Because HER3 remained highly phosphorylated without treatment in PC9AZDR7 cells and osimertinib inhibited HER3 phosphorylation, we next hypothesized that PC9AZDR7 cells maintain HER3 function. We compared the anticancer effect of U3-1402 in PC9AZDR7 and parental PC9 cells using a xenograft tumour model. These cell lines were implanted subcutaneously in mice, which were then treated with a reduced single dose of U3-1402 (3 mg/kg) administered i.p. or with vehicle for 21 days. Xenograft tumours arising from PC9 parent cells were not significantly reduced by U3-1402 administration with a T/C ratio of 83% on day 21 (Fig. 4c). However, growth of tumours originating from PC9AZDR7 cells was notably prevented by U3-1402 treatment (T/C ratio of 28%) on day 18 ($p = 0.01$; Fig. 4c). These results indicate that the anticancer activity of U3-1402 may increase in PC9 cells after acquiring resistance to osimertinib.

Osimertinib-resistant PC9AZDR7 cells are sensitive to U3-1402 via HER3 re-localization to the plasma membrane

Immunoblotting revealed that HER3 expression in whole-cell lysates was comparable between parent PC9 and PC9AZDR7 cells (Fig. 4b). However, based on our findings in HCC827GR5 cells, in which HER3 expression on the cell surface is correlated with U3-1402 efficacy, we measured and compared cell surface HER3 expression levels between PC9 and PC9AZDR7 cells. Flow cytometry revealed that PC9 cells have approximately 5088 HER3 molecules per cell, whereas PC9AZDR7 cells have approximately three times as many, at 15,469 HER3 molecules per cell ($p < 0.001$; Fig. 4d). Immunofluorescence staining also demonstrated greater cell surface HER3 expression in PC9AZDR7 cells than in PC9 cells (Fig. 4e).

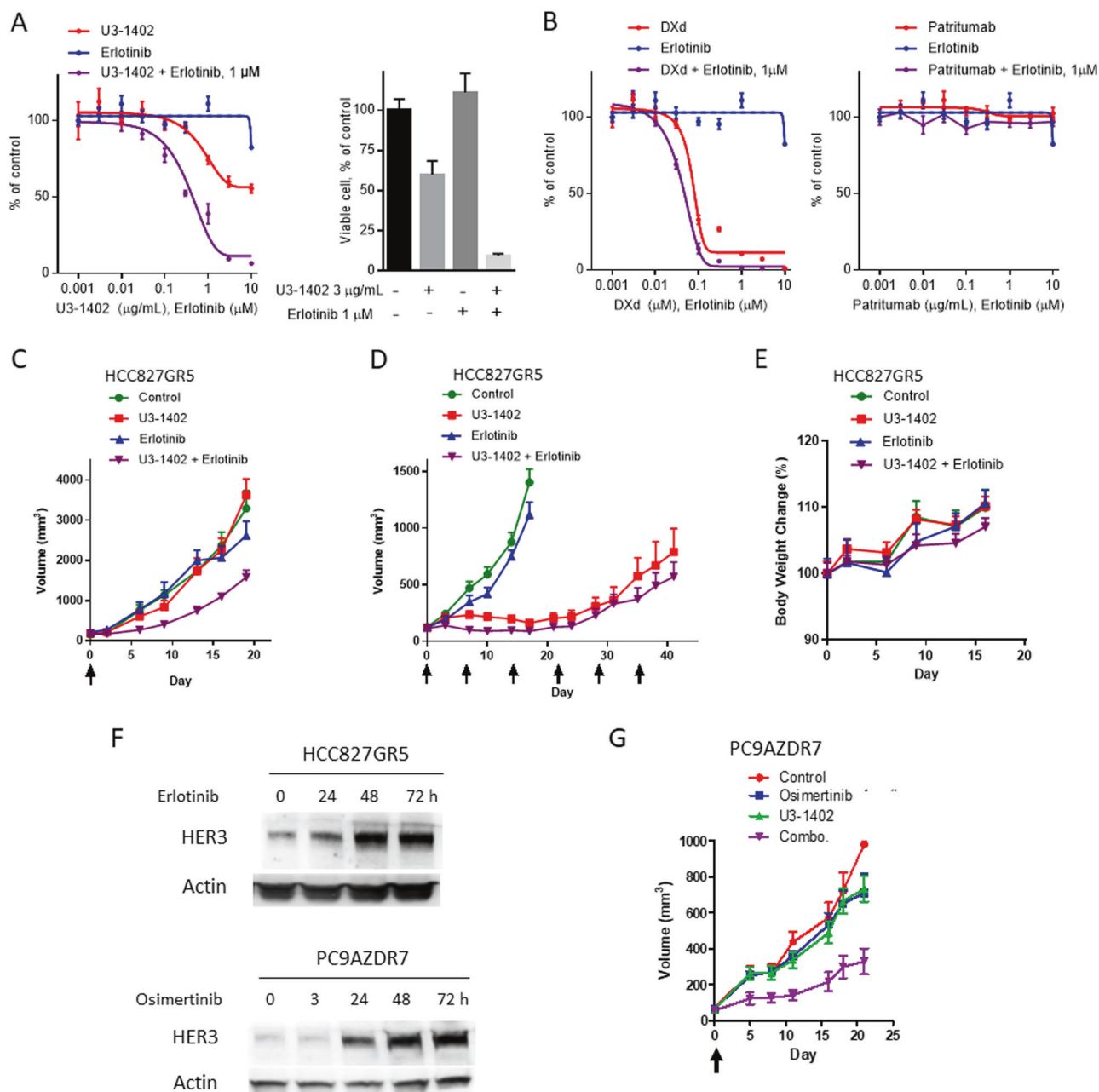


Fig. 5 **a** In vitro growth inhibition assay for U3-1402 in combination with erlotinib. HCC827GR5 cells were treated with the indicated concentrations of U3-1402, erlotinib, or U3-1402 plus 1 μ M erlotinib for 7 days; cell viability was evaluated using the CellTiter-Glo viability assay and is shown relative to untreated control cells (mean \pm SD of six independent experiments). **b** In vitro growth inhibition assay for U3-1402, patritumab, and DXd alone or in combination with 1 μ M erlotinib. HCC827GR5 cells were treated with the indicated drugs for 7 days; cell viability was evaluated using the CellTiter-Glo viability assay and is shown relative to untreated control cells (mean \pm SD of six independent experiments). **c**, **d** In a xenograft HCC827GR5 mouse model, tumours were treated with either (c) U3-1402 alone (3 mg/kg triweekly) or (d) U3-1402 alone (10 mg/kg weekly) in addition to

erlotinib (25 mg/kg), U3-1402 in combination with erlotinib, or vehicle. Each treatment group consisted of eight or ten mice. Data represent mean \pm SEM. The vertical arrow indicates drug administration. **e** Body weight change of host mice after treatment with U3-1402 (10 mg/kg weekly), erlotinib (25 mg/kg), both drugs in combination, or vehicle. Values shown are mean \pm SD ($n = 10$). **f** HCC827GR5 or PC9AZDR7 cells were treated with 1 μ M erlotinib or 100 nM osimertinib for 72 h. HER3 and actin proteins were detected by immunoblotting. **g** In a xenograft PC9AZDR7 mouse model, tumours were treated with either a single dose of U3-1402 (1 mg/kg) or osimertinib (1 mg/kg) alone, both drugs in combination, or vehicle. Each treatment group consisted of 8, 10, or 12 mice. Data represent mean \pm SEM. The vertical arrow indicates drug administration

Additionally, we assessed intracellular HER3 localization using immunofluorescent microscopy. As reported

previously [7, 19–22], HER3 is predominantly located intracellularly rather than on the cell membrane. In PC9

cells, HER3 was largely expressed in the nucleus with minimal localization in the cytoplasm (Fig. 4f), whereas in PC9AZDR7 cells, HER3 was localized in the nucleus was reduced, and HER3 was predominantly found in vesicles in the cytoplasm (Fig. 4f). These observations suggest that the greater anticancer efficacy of U3-1402 in osimertinib-resistant PC9AZDR7 cells may be achieved by increased cell surface HER3 expression in PC9AZDR7 cells compared with that in parental PC9 cells. In addition, altered localization of HER3 may indicate aberrant HER3 trafficking in PC9AZDR7 cells. Thus, changes to HER3-U3-1402 complex trafficking may result in increased DXd cleavage in cytoplasmic lysosomes.

U3-1402 combined with erlotinib potently inhibits xenograft tumour growth in erlotinib-resistant HCC827GR5 cells

Although U3-1402 treatment alone was effective against EGFR-TKI-resistant NSCLC, we also examined the effect of cotreatment using U3-1402 and an EGFR-TKI in HCC827GR5 cells. Using an *in vitro* growth inhibition assay with HCC827GR5 cells, we evaluated the anticancer efficacy of erlotinib at doses of 0.0033–10 μM and U3-1402 at doses of 0.0033–10 $\mu\text{g/mL}$, both alone and in combination, for 7 days. Erlotinib treatment alone did not decrease the viability of HCC827GR5 cells ($\text{IC}_{50} > 10 \mu\text{M}$) and exerted no inhibitory effects on cell growth at 1 μM (Fig. 5a), whereas U3-1402 treatment alone dose-dependently decreased cell viability, reaching 60% of control values at a concentration of 3 $\mu\text{g/mL}$ (Fig. 5a). Notably, the combination of U3-1402 with 1 μM erlotinib significantly decreased HCC827GR5 cell viability to a greater extent than either drug alone, reaching 9% of control values at concentrations of 3 $\mu\text{g/mL}$ for U3-1402 and 1 μM for erlotinib (Fig. 5a). We also evaluated the anticancer effects of patritumab plus 1 μM erlotinib or of DXd plus 1 μM erlotinib for 7 days at the indicated concentrations but did not observe a synergistic effect (Fig. 5b).

To determine whether these effects apply *in vivo*, the antitumorigenic potential of this drug combination was evaluated in mice with HCC827GR5 xenografts. Neither daily *p.o.* of erlotinib (25 mg/kg) nor a reduced triweekly dose of *i.p.* administered U3-1402 (3 mg/kg) alone affected tumour growth, with T/C ratios of 79% and 110% on day 19 (Fig. 1c). However, administration of both drugs in combination significantly suppressed tumour growth compared with that found in control mice on day 19 with a T/C ratio of 48% ($p = 0.006$; Fig. 5c). Additionally, increasing the dose of *i.p.* administered U3-1402 to 10 mg/kg weekly combined with 25 mg/kg *p.o.* administered erlotinib daily resulted in significantly improved T/C ratios compared with those of other groups on days 7, 10, and 14 ($p < 0.005$) and

maintained anticancer efficacy (Fig. 5d). A previous study showed that ADC payload release in plasma caused toxicity in the host [13]. Therefore, we evaluated the effect of U3-1402 on mouse body weight during treatment. There was no significant body weight loss following either treatment with 10 mg/kg U3-1402 (*i.p.* weekly administration), alone or in combination with erlotinib.

To elucidate the synergistic efficacy of the U3-1402 and erlotinib combination in HCC827GR5 cells, HER3 expression was analysed in erlotinib-treated HCC827GR5 cells over 72 h by immunoblotting. Intriguingly, we observed that erlotinib increased HER3 expression in HCC827GR5 cells after 24 h in a time-dependent manner (Fig. 5f). Furthermore, we found that osimertinib also increased HER3 expression in osimertinib-resistant PC9AZDR7 cells after 3 h of osimertinib exposure (Fig. 5f). Additionally, the combination of osimertinib (1 mg/kg) and U3-1402 (low dose, 1 mg/kg) had a synergistic effect in PC9AZDR7 cells (Fig. 5g). These findings indicate that EGFR-TKI and U3-1402 combination therapy may exhibit synergistic efficacy due to EGFR-TKI-mediated upregulation of HER3.

Discussion

The HER3-targeted ADC U3-1402 is currently under clinical development and requires biomarkers for identifying the optimal patient population for treatment [12]. In the current study, we report for the first time that U3-1402 is an effective treatment for EGFR-mutant NSCLC despite its EGFR-TKI resistance. Additionally, administration of U3-1402 in combination with an EGFR-TKI was more potent than treatment with U3-1402 alone in EGFR-TKI-resistant cells. Although EGFR-TKIs are the current standard therapy for patients with EGFR-mutant NSCLC, patients eventually develop acquired resistance, and optimal management strategies for patients with acquired resistance to EGFR-TKIs remain poorly defined [23]. Clinical examination showed that treatment with the anti-HER3 antibody patritumab in combination with erlotinib achieved no objective response in five patients with EGFR-mutant NSCLC with acquired resistance to EGFR-TKI [11]. Consistent with previous studies [6], HCC827GR5 cells were resistant to the anti-HER3 antibody patritumab, whereas anticancer efficacy was markedly enhanced by drug conjugation to an anti-HER3 antibody. A number of molecular alterations, such as EGFR secondary mutations, *MET* genomic amplification, and *HER2* genomic amplification, heterogeneously cause EGFR-TKI resistance in EGFR-mutant NSCLC [5, 16, 23–25]. Nevertheless, U3-1402 is a potentially viable treatment for a heterogeneous population of EGFR-TKI-resistant NSCLC with HER3 expression.

Furthermore, U3-1402 is expected to be well tolerated by the host, as we observed in a xenograft mouse model that body weight loss was minimal despite receiving high doses of U3-1402. A previous study has shown that the payload from ADCs is released in plasma, and that this free payload in plasma causes dose-limiting toxicities, such as thrombocytopenia, neutropenia, and neuropathy [26]. In contrast to the drug linker system for these ADCs, the drug linker system for U3-1402 and DS-8201, which is a HER2-targeted ADC, is unique in its reduced toxicity. Furthermore, a clinical trial of the HER2 ADC DS-8201a for patients with HER2-positive breast and gastric cancer demonstrated that DS-8201a is stable in plasma and has preferable pharmacokinetics despite its high DAR [27]. Therefore, U3-1402 is anticipated to be stable in plasma and may clinically be a less toxic treatment option.

Unexpectedly, we observed increased susceptibility to U3-1402 in EGFR-TKI-resistant cells, especially in the PC9AZDR7 xenograft model, compared with their parent cells. Additionally, U3-1402 caused potent DNA damage in EGFR-TKI-resistant HCC827GR5 cells rather than blocking the HER3/PI3K/AKT signalling pathway. The improved efficacy of U3-1402 may be mediated by increased cell surface HER3 expression in EGFR-TKI-resistant cells, in which U3-1402 internalization is increased compared with that in parent cells. This may result in an increase in DXd in the cytoplasm of HCC827GR5 cells, which induces potent DNA damage. The efficacy of a number of ADCs is significantly correlated with antigen expression level in cancer cells [13, 28–30]. Similarly, the efficacy of U3-1402 is correlated with increased expression of cell surface HER3 in breast cancer cells [12]. Thus, EGFR-mutant NSCLC with increased cell surface HER3 expression may exhibit increased sensitivity to U3-1402. We did not elucidate the mechanism that underlies these observed changes in efficacy with changes in cell surface HER3 expression levels. However, Sergina et al. reported that EGFR-TKI-induced HER3 re-localization to the plasma membrane, which was driven by the loss of AKT signalling, likely involved AKT-mediated negative feedback signalling [7]. We found that exposure of osimertinib-resistant PC9AZDR7 cells to osimertinib also partially decreased AKT phosphorylation, which may induce cell surface HER3 localization.

Alternatively, intracellular trafficking of the HER3-U3-1402 complex may influence the efficacy of U3-1402. As DXd release in the cytosol occurs only following linker-payload cleavage in lysosomes, efficient lysosomal degradation of U3-1402 is essential for its effective action. In the current study, HER3 was predominantly located in the nucleus of PC9 cells, although it was localized in the cytoplasm of PC9AZDR7 cells. Thus, we proposed that HER3 trafficking to the nucleus was decreased in PC9AZDR7 cells, and this alteration may also potentially change HER3-U3-1402

complex trafficking. In PC9AZDR7 cells, U3-1402 likely undergoes accelerated cleavage by lysosomal enzymes, which are localized in the cytoplasm, and the resulting free DXd causes DNA damage. It has been reported that HER3 is localized in the nucleus in some types of cancer cells [19–22] and that ErbB3 nuclear translocation is a common event in proliferating tissues [19]. Future investigations are warranted to elucidate the mechanisms of HER3 trafficking to the nucleus in EGFR-mutant NSCLC.

The current study demonstrates the efficacy of U3-1402 in NSCLC with acquired resistance to EGFR-TKIs. We recommend that administration of U3-1402 alone or in combination with an EGFR-TKI should be evaluated in a clinical setting with a patient cohort with TKI-refractory NSCLC tumours and EGFR-activating mutations.

Materials and methods

Cells and reagents

EGFR-mutant NSCLC cell lines PC9 and HCC827 were obtained from the American Type Culture Collection (Manassas, VA, USA), and EGFR-TKI gefitinib-resistant HCC827GR5 cells were kindly provided by Dr. Pasi A. Jänne (Dana-Farber Cancer Institute, Boston, MA, USA) [5]. Authenticity of the cells was regularly tested by short tandem repeat (STR). All cell lines were previously characterized [5, 6]. Cells were maintained in a humidified atmosphere of 5% CO₂ at 37 °C in RPMI-1640 medium (Sigma-Aldrich, St. Louis, MO, USA) supplemented with 10% fetal bovine serum (FBS) and 1% penicillin streptomycin. Erlotinib and osimertinib were obtained from commercial sources. U3-1402, patritumab, and DXd were provided by Daiichi Sankyo Co., Ltd (Tokyo, Japan).

In vitro growth inhibition assay

Cells were plated in 96-well round-bottomed plates at 1×10^4 cells/well in RPMI-1640 medium containing 2% FBS. After 24 h of incubation, U3-1402, erlotinib, osimertinib, patritumab, and DXd were added at various concentrations. Following a 7-day incubation, cell viability was assessed by CellTiter-Glo Luminescent Cell Viability Assay (Promega, Madison, WI, USA). Luminescence values are expressed as percentages of that observed in untreated cells, and the IC₅₀ of each drug was calculated.

Antibodies and western blotting

Cells were seeded at a density of 1×10^6 cells/plate in Prime Surface 60-mm plates (Sumitomo Bakelite Co. Ltd, Tokyo, Japan) and allowed to grow overnight in medium containing

0.5% FBS before the addition of drugs. Cells were incubated for different durations and then harvested. Western blotting was performed as previously described [6]. Proteins were probed with antibodies against phospho-AKT, AKT, phospho-EGFR, EGFR, phospho-HER3, and HER3 (all from Cell Signaling Technology, Danvers, MA, USA) and phospho-ERK1/2 (Santa Cruz Biotechnology, Santa Cruz, CA, USA).

Reverse transcription and real-time PCR

Total RNA was isolated from cells using the RNeasy Mini Kit (Qiagen, Valencia, CA, USA), according to the manufacturer's instructions. Complementary DNA (cDNA) was synthesized using a High Capacity RNA-to-cDNA Kit (Applied Biosystems, Carlsbad, CA, USA) and used for RT-PCR to measure *HER3* expression, with glyceraldehyde-3-phosphate dehydrogenase (*GAPDH*) as an internal standard. Expression levels were determined using a standard method with an ABI 7900 HT system and SDS software (Applied Biosystems).

In vivo tumour growth inhibition assay

All animal experiments were performed in accordance with the Recommendations for Handling of Laboratory Animals for Biomedical Research compiled by the Committee on Safety and Ethical Handling Regulations or Laboratory Animal Experiments of Kindai University. The study was also reviewed and approved by the Animal Ethics Committee of Kindai University. HCC827, HCC827GR5, PC9, or PC9AZDR7 cells (5×10^6 cells/mouse) were subcutaneously injected into the right flanks of female BALB/cA Jcl-nu/nu mice (CLEA Japan, Tokyo, Japan). Once tumours had reached the target volume (0.2 cm^3), mice were randomly assigned to treatment and control groups. Mice received a single or weekly i.p. injection of PBS (100 μL ; control), patritumab (10 mg/kg body weight in 100 μL phosphate-buffered saline (PBS)), or U3-1402 (3 or 10 mg/kg body weight in 100 μL PBS), or daily p.o. administration of erlotinib (25 mg/kg body weight in 100 μL PBS). Tumour volumes and mouse body weights were measured twice per week. Mice were sacrificed if tumours became necrotic or grew to a volume of 2.0 cm^3 . Tumour volume was defined as $1/2 \times \text{length} \times \text{width}^2$. The T/C ratio was calculated according to the following equation: $100 \times (\text{average tumour volume of the treated group}) / (\text{average tumour volume of the control group})$. The PDX, TM00784, was provided by Jackson Laboratory (Bar Harbor, ME, USA).

Antigen expression analysis by flow cytometry

Quantification of cell surface antigens was carried out using QIFIKIT (Dako, Tokyo, Japan). Each cell line was treated

with a saturating concentration of mouse anti-HER3 antibody (clone 1B4C3) or mouse IgG2a isotype control, followed by staining with an fluorescein isothiocyanate-conjugated (FITC) anti-mouse IgG (Dako). Each sample was analysed by LSRFortessa X-20 (BD Biosciences, San Jose, CA, USA), and the number of binding sites per cell was calculated according to the manufacturer's instructions.

Immunofluorescence

Immunofluorescence was performed using a Duolink In Situ immunoassay (Sigma-Aldrich) according to the manufacturer's instructions. Cell samples were incubated with a blocking solution, followed by incubation with primary antibodies: a mouse monoclonal anti-HER3 extracellular domain antibody (GeneTex, Irvine, CA, USA) and a polyclonal rabbit anti-HER3 C-terminus antibody (Santa Cruz Biotechnology). Samples were mixed with proximity ligation assay (PLA) probes (Sigma-Aldrich) and incubated followed by the addition of ligation solution. Samples were mounted with Duolink In Situ Mounting Medium with 4,6-diamidino-2-phenylindole (DAPI) and analysed using a fluorescent microscope (Keyence, Osaka, Japan). When only cell surface HER3 was evaluated, cell surface permeation was not performed.

Statistical analysis

Statistical analysis was performed using SPSS version 22.0 (IBM Corp., Armonk, NY, USA). All statistical tests were two-sided, unpaired *t*-tests, and *p*-values < 0.05 were considered statistically significant. Data were graphically depicted using GraphPad Prism 5.0 for Windows (GraphPad Software, Inc., La Jolla, CA, USA).

Acknowledgements We thank Haruka Yamaguchi, Yume Shinkai, and Michiko Kitano for technical support.

Compliance with ethical standards

Conflict of interest Dr. Yonesaka and Dr. Nakagawa received research funding from Daiichi Sankyo Co., Ltd., and Dr. Maeda, Dr. Kagari, and Dr. Hirotani are employees of Daiichi Sankyo Co., Ltd. The remaining authors declare that they have no conflict of interest.

Financial support This study was financially supported by Daiichi Sankyo Co., Ltd. U3-1402 and patritumab were provided by Daiichi Sankyo Co., Ltd.

References

1. Campbell MR, Amin D, Moasser MM. HER3 comes of age: new insights into its functions and role in signalling, tumour biology, and cancer therapy. *Clin Cancer Res*. 2010;16:1373–83.

2. Yi ES, Harclerode D, Gondo M, Stephenson M, Brown RW, Younes M, et al. High c-erbB-3 protein expression is associated with shorter survival in advanced non-small cell lung carcinomas. *Mod Pathol.* 1997;10:142–8.
3. Cappuzzo F, Toschi L, Domenichini I, Bartolini S, Ceresoli GL, Rossi E, et al. HER3 genomic gain and sensitivity to gefitinib in advanced non-small-cell lung cancer patients. *Br J Cancer.* 2005;93:1334–40.
4. Engelman JA, Jänne PA, Mermel C, Pearlberg J, Mukohara T, Fleet C, et al. ErbB-3 mediates phosphoinositide 3-kinase activity in gefitinib-sensitive non-small cell lung cancer cell lines. *Proc Natl Acad Sci USA.* 2005;102:3788–93.
5. Engelman JA, Zejnullahu K, Mitsudomi T, Song Y, Hyland C, Park JO, et al. MET amplification leads to gefitinib resistance in lung cancer by activating ERBB3 signalling. *Science.* 2007;316:1039–43.
6. Yonesaka K, Hirotani K, Kawakami H, Takeda M, Kaneda H, Sakai K, et al. Anti-HER3 monoclonal antibody patritumab sensitizes refractory non-small cell lung cancer to the epidermal growth factor receptor inhibitor erlotinib. *Oncogene.* 2016;35:878–86.
7. Sergina NV, Rausch M, Wang D, Blair J, Hann B, Shokat KM, et al. Escape from HER-family tyrosine kinase inhibitor therapy by the kinase-inactive HER3. *Nature.* 2007;445:437–41.
8. Mendell J, Freeman DJ, Feng W, Hettmann T, Schneider M, Blum S, et al. Clinical translation and validation of a predictive biomarker for patritumab, an anti-human epidermal growth factor receptor 3 (HER3) monoclonal antibody, in patients with advanced non-small cell lung cancer. *EBioMedicine.* 2015;2:264–71.
9. Meulendijks D, Jacob W, Voest EE, Mau-Sorensen M, Martinez-Garcia M, Taus A, et al. Phase Ib study of lumretuzumab plus cetuximab or erlotinib in solid tumour patients and evaluation of HER3 and heregulin as potential biomarkers of clinical activity. *Clin Cancer Res.* 2017. <https://doi.org/10.1158/1078-0432.CCR-17-0812>.
10. Juric D, Dienstmann R, Cervantes A, Hidalgo M, Messersmith W, Blumenschein GR, et al. Safety and pharmacokinetics/pharmacodynamics of the first-in-class dual action HER3/EGFR antibody MEHD7945A in locally advanced or metastatic epithelial tumours. *Clin Cancer Res.* 2015;21:2462–70.
11. Shimizu T, Yonesaka K, Hayashi H, Iwasa T, Haratani K, Yamada H, et al. Phase 1 study of new formulation of patritumab (U3-1287) Process 2, a fully human anti-HER3 monoclonal antibody in combination with erlotinib in Japanese patients with advanced non-small cell lung cancer. *Cancer Chemother Pharmacol.* 2017;79:489–95.
12. Ueno S, Hirotani K, Abraham R, Blum S, Frankenberger B, Redondo-Muller M, et al. U3-1402, a novel HER3-targeting ADC with a novel DNA topoisomerase I inhibitor, demonstrates a potent anti-tumour efficacy. *Cancer Res.* 2017;77(Suppl 13):3092. <https://doi.org/10.1158/1538-7445.AM2017-3092>.
13. Ogitani Y, Aida T, Hagihara K, Yamaguchi J, Ishii C, Harada N, et al. DS-8201a, a novel HER2-targeting ADC with a novel DNA topoisomerase I inhibitor, demonstrates a promising antitumor efficacy with differentiation from T-DM1. *Clin Cancer Res.* 2016;22:5097–108.
14. Takegawa N, Nonagase Y, Yonesaka K, Sakai K, Maenishi O, Ogitani Y, et al. DS-8201a, a new HER2-targeting antibody-drug conjugate incorporating a novel DNA topoisomerase I inhibitor, overcomes HER2-positive gastric cancer T-DM1 resistance. *Int J Cancer.* 2017. <https://doi.org/10.1002/ijc.30870>.
15. Zhou C, Yao LD. Strategies to improve outcomes of patients with EGFR-mutant non-small cell lung cancer: review of the literature. *J Thorac Oncol.* 2016;11:174–86.
16. Kobayashi S, Boggon T, Dayaram T, Jänne PA, Kocher O, Meyerson M, et al. EGFR mutation and resistance of non-small cell lung cancer to gefitinib. *N Engl J Med.* 2005;352:786–92.
17. Jänne PA, Yang JCH, Kim DW, Planchard D, Ohe Y, Ramalingam SS, et al. AZD9291 in EGFR inhibitor-resistant non-small-cell lung cancer. *N Engl J Med.* 2015;372:1689–99.
18. Yonesaka K, Zejnullahu K, Okamoto I, Satoh T, Cappuzzo F, Souglakos J, et al. Activation of ERBB2 signalling causes resistance to the EGFR-directed therapeutic antibody cetuximab. *Sci Transl Med.* 2011;3:99ra86.
19. Reif R, Adawy A, Vartak N, Schröder J, Günther G, Ghallab A, et al. Activated ErbB3 translocates to the nucleus via clathrin-independent endocytosis, which is associated with proliferating cells. *J Biol Chem.* 2016;291:3837–47.
20. Offterdinger M, Schöfer C, Weipoltshammer K, Grunt TW. c-erbB-3: a nuclear protein in mammary epithelial cells. *J Cell Biol.* 2002;157:929–39.
21. Begnami MD, Fukuda E, Fregnani JH, Nonogaki S, Montagnini AL, da Costa WL, et al. Prognostic implications of altered human epidermal growth factor receptors (HERs) in gastric carcinomas: HER2 and HER3 are predictors of poor outcome. *J Clin Oncol.* 2011;29:3030–6.
22. Trocme E, Mougiakakos D, Johansson CC, All-Eriksson C, Economou MA, Larsson O, et al. Nuclear HER3 is associated with favorable overall survival in uveal melanoma. *Int J Cancer.* 2012;130:1120–7.
23. Sequist LV, Waltman BA, Dias-Santagata D, Digumarthy S, Turke AB, Fidias P, et al. Genotypic and histological evolution of lung cancers acquiring resistance to EGFR inhibitors. *Sci Transl Med.* 2011;3:75ra26.
24. Jia Y, Yun CH, Park E, Ercan D, Manuia M, Juarez J, et al. Overcoming EGFR(T790M) and EGFR(C797S) resistance with mutant-selective allosteric inhibitors. *Nature.* 2016;534:129–32.
25. Takezawa K, Pirazzoli V, Arcila ME, Nebhan CA, Song X, de Stanchina E, et al. HER2 amplification: a potential mechanism of acquired resistance to EGFR inhibition in EGFR-mutant lung cancers that lack the second-site EGFR T790M mutation. *Cancer Discov.* 2012;2:922–33.
26. Loganzo F, Sung M, Gerber HP. Mechanisms of resistance to antibody-drug conjugates. *Mol Cancer Ther.* 2016;15:2825–34.
27. Doi T, Iwata H, Tsurutani J, Takahashi S, Park H, Redfern CH, et al. Single agent activity of DS-8201a, a HER2-targeting antibody-drug conjugate, in heavily pretreated HER2 expressing solid tumours. *J Clin Oncol.* 2017;35(Suppl 15):108. https://doi.org/10.1200/JCO.2017.35.15_suppl.108
28. Burris HA 3rd, Rugo HS, Vukelja SJ, Vogel CL, Borson RA, Limentani S, et al. Phase II study of the antibody drug conjugate trastuzumab-DM1 for the treatment of human epidermal growth factor receptor 2 (HER2)-positive breast cancer after prior HER2-directed therapy. *J Clin Oncol.* 2011;29:398–405.
29. Chen R, Hou J, Newman E, Kim Y, Donohue C, Liu X, et al. CD30 downregulation, MMAE resistance, and MDR1 upregulation are all associated with resistance to brentuximab vedotin. *Mol Cancer Ther.* 2015;14:1376–84.
30. Loganzo F, Tan X, Sung M, Jin G, Myers JS, Melamud E, et al. Tumor cells chronically treated with a trastuzumab-maytansinoid antibody-drug conjugate develop varied resistance mechanisms but respond to alternate treatments. *Mol Cancer Ther.* 2015;14:952–63.